Journal of Applied Geophysics 230 (2024) 105522

Contents lists available at ScienceDirect

Journal of Applied Geophysics

journal homepage: www.elsevier.com/locate/jappgeo

Investigating the relationships between radon and the geology of the Sterkfontein cave

Jacques Bezuidenhout *, Rikus le Roux

Faculty of Military Science, Stellenbosch University, South Africa

ARTICLE INFO

Keywords:
Radon
Cave
Sterkfontein
Geology
QGIS
Karstic cave

ABSTRACT

Radon, a naturally occurring radioactive gas, has become a subject of increasing interest and concern, particularly in the context of subterranean environments such as caves. This research investigates these dynamics in the Sterkfontein Cave in South Africa, which has formed in the karst geology of the Cradle of Humankind, Gauteng. Additionally, it set out to compile a radon map for the cave, identifying potential radon hotspots. Twenty-four electret ion chambers were placed in the tourist section of the cave and left for a period of 24 h. The radon concentrations were found to be between 53 Bq/m^3 and 2770 Bq/m^3. Three regions within the cave exhibited elevated radon concentrations, with these occurrences being linked to phosphatic deposits. A subterranean lake also concentrates radon gas in the lower areas of the cave. While the cave's average radon concentration of 427 Bq/m^3 exceeds the World Health Organization's (WHO) hazardous level of 300 Bq/m^3, occupational exposure remains minimal during a typical cave tour. Consequently, there is no discernible risk during an average tour through the cave.

1. Background

Enclosed environments in caves can result in the build-up of radon gas and the risk of exposure. Radon in caves has consequently been studied for many years, and a substantial quantity of information is available on the behaviour of this gas in cave systems. In general, carbon dioxide and radon concentrations positively correlate in caves, which renders them useful tracers for cave climate and ventilation studies (Cigno, 2005). However, prior research has mainly concentrated on caves with carbonate lithologies, resulting in karst landscapes receiving the most attention. The Sterkfontein area in South Africa is dominated by dolomite lithology, but several other rock units are also represented in the Sterkfontein Cave.

The Sterkfontein Cave lies within the Cradle of Humankind World Heritage Site in the north-west of the Gauteng Province, South Africa. The Cradle earned World Heritage Site status due to its fossil- and artefact-bearing landscape-exposed palaeocave infills, which formed within karstified dolomitic limestone. The Sterkfontein Cave represents one of the richest hominin-bearing sites in the world, with over 800 specimens being recovered from excavations of the landscape-exposed palaeocave infills and deposits that are preserved in the underground network. Notable discoveries at Sterkfontein include: TM1511, the first adult Australopithecus specimen; Mrs. Ples, which was the most complete Australopithecus cranium until the discovery of Little Foot, StW 573; three partial Australopithecus skeletons, the most complete early hominin skeleton discovered to date (Thackeray, 2020).

The karstic cave with chert bands and occasional shale beds developed within the dolomite of the Transvaal Supergroup (Wilkinson, 1983) (Eriksson and Reczko, 1995). The dolomite was formed as part of a carbonate ramp sedimentary environment and is overlain by the Transvaal sequence. The present-day cave, which is partly infilled, were created around 20 million years ago and were only revealed to the surface approximately 5 million years ago (Stratford, 2015). Within the cave, there are sediments containing fossils and artefacts from the Plio-Pleistocene period, which are distinct from the sedimentary history of the host rock. The fossiliferous breccia accumulated at talus cones in underground cavities through the deposition of sediments introduced through avens-style openings in the cave ceilings (Wipplinger et al., 2003). Opening of the cave to the surface occurs through localized meteoric denudation at faults and collapses in the vadose zone. There are 25 such openings and some are often deep and even connect the surface directly to the base of the cave (Kuman, 1994).

The Sterkfontein Cave lies beneath the Swartkrans hill on the south side of the north-west flowing Blaaubank River, which springs from the

* Corresponding author.
E-mail address: jb@sun.ac.za (J. Bezuidenhout).

https://doi.org/10.1016/j.jappgeo.2024.105522
Received 15 March 2024; Received in revised form 12 September 2024; Accepted 13 September 2024
Available online 14 September 2024

Witwatersrand ridge. The Sterkfontein Cave tourist section contains four largely northwest to southeast-facing chambers, the largest of which are the Milner Hall (Gallery A in Fig. 1) and the Elephant Chamber (Gallery B in Fig. 1), that slope downwards toward the Blaaubank River (Fig. 1). These chambers are joined by interconnecting tunnels and share a subterranean lake. The highest subterranean section of the cave is the Exit series of tunnels leading and the Graveyard Chambers (Gallery C in Fig. 1). Many of the cave's natural openings to the surface were influenced by the structural geology of the cave. Several of its modern openings, however, are a combination of natural and anthropogenic entrances. The tourist section of the Sterkfontein cave covers only about 15 % of the accessible system. The remainder of the known cave, which cumulatively adds up to about 5 km of passages and chambers, is only accessible to researchers and palaeontologists.

According to the National Council on Radiation Protection and Measurements (NCRP), approximately 10 % of the radon produced within the initial meter of soil that is exposed to the atmosphere eliminates into the atmosphere (NCRP, 1988). Two mechanisms, namely diffusion and gas transport, enable radon to escape from unexposed soil and rock. The diffusion rate is determined by intergranular channels, capillaries, and smaller pores. The transport rate depends on the porosity and cracks in the soil, sediment, or exposed rock, which makes this process more prevalent in fractured soil or rocks with higher surface areas (Tanner, 1978). Clastic sediments that have accumulated in the cave, along with large areas of exposed host rock within the cave system, can therefore significantly support radon diffusion and transport.

Radon concentrations are influenced by several factors, which include air and water flow, atmospheric pressure, seismic activity, anthropogenic and biogenic activities, as well as seasonality. Seasonal trends of radon generation and accumulation in caves generally peak in summer and reduce in winter (Hakl et al., 1997). The density difference between the air in cave cavities and the air outside causes cave breathing. These density differences result from variations in temperature and air pressure. Generally, the vadose zone of karstic caverns, such as at Sterkfontein, has a fractured structure that regulates cave ventilation patterns (Gabrovsek, 2023). When studying radon within a cave, it is therefore important to consider the varying ventilation patterns of different cave systems.

This research explores the unique dynamics of radon distribution within the tourist section of the Sterkfontein Cave and examines the potential causes for radon concentration variations. A key contribution of this study is the creation of detailed radon concentration maps for the cave, which highlights potential radon hotspots and offers new insights into radon behaviour in such complex subterranean environments. This mapping provides valuable data that can inform both geological studies and public health considerations related to radon exposure.

2. Method

2.1. Radon measurements

Electret ion chambers (EICs) from Rad-Elec Inc., called *E*-PERM™, were utilized to measure the radon levels in various areas of the cave, predominantly along the tourist route. Before entering the cave, the starting potential of each electret was measured using a surface potential electret voltage reader (SPER), also from Rad-Elec Inc. The electrets were distributed throughout the cave by placing the EICs in 24 locations, as shown in Fig. 2. These locations were selected based on their occupancy by tourists and guides, surrounding geology, ventilation, and potential to accumulate radon. The EICs were deployed starting from the Tourist Entrance, working in a clockwise direction through the cave toward the Tourist Exit. In each of these locations, the EICs were placed

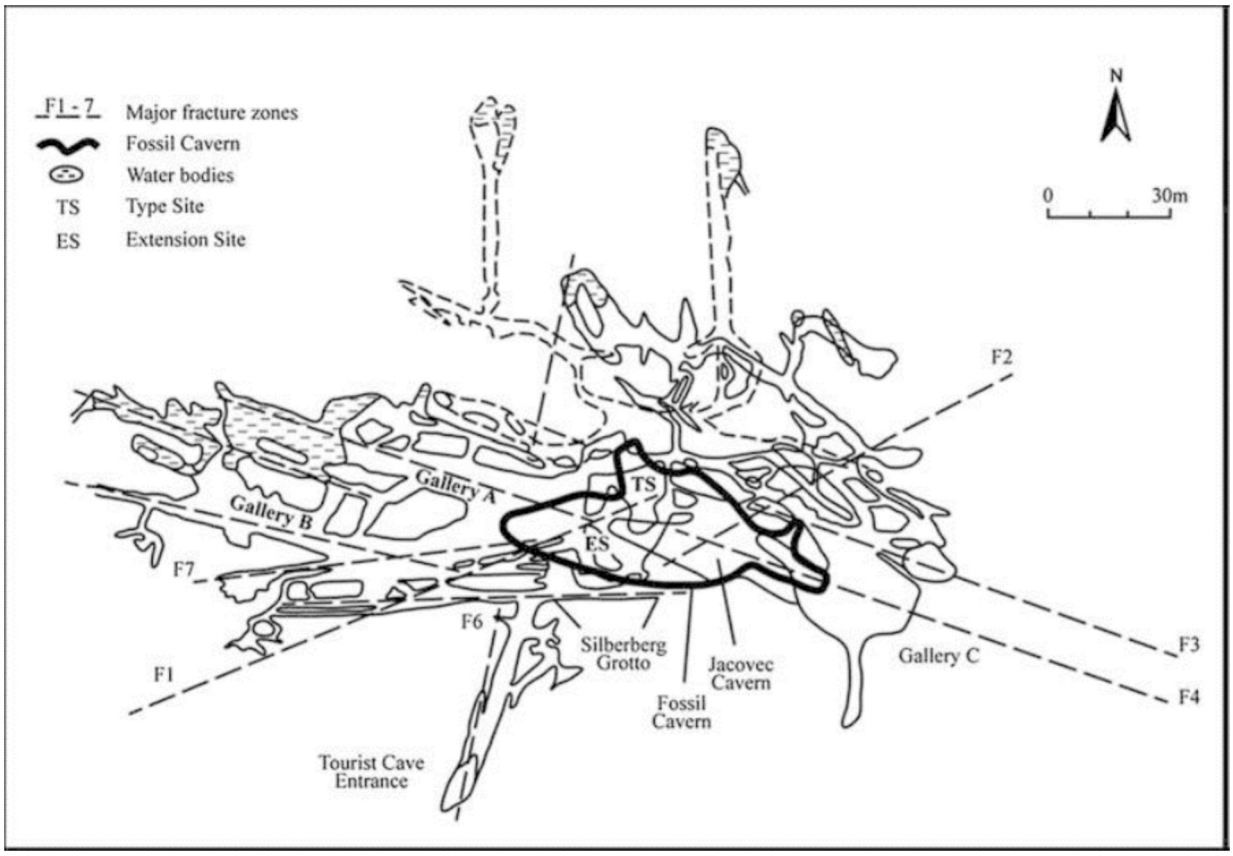

Fig. 1. Geomorphological map of the Sterkfontein Cave indicating the faults and cavities. The upper-level fossil cavern is shown with a bold black line (Stratford, 2017).

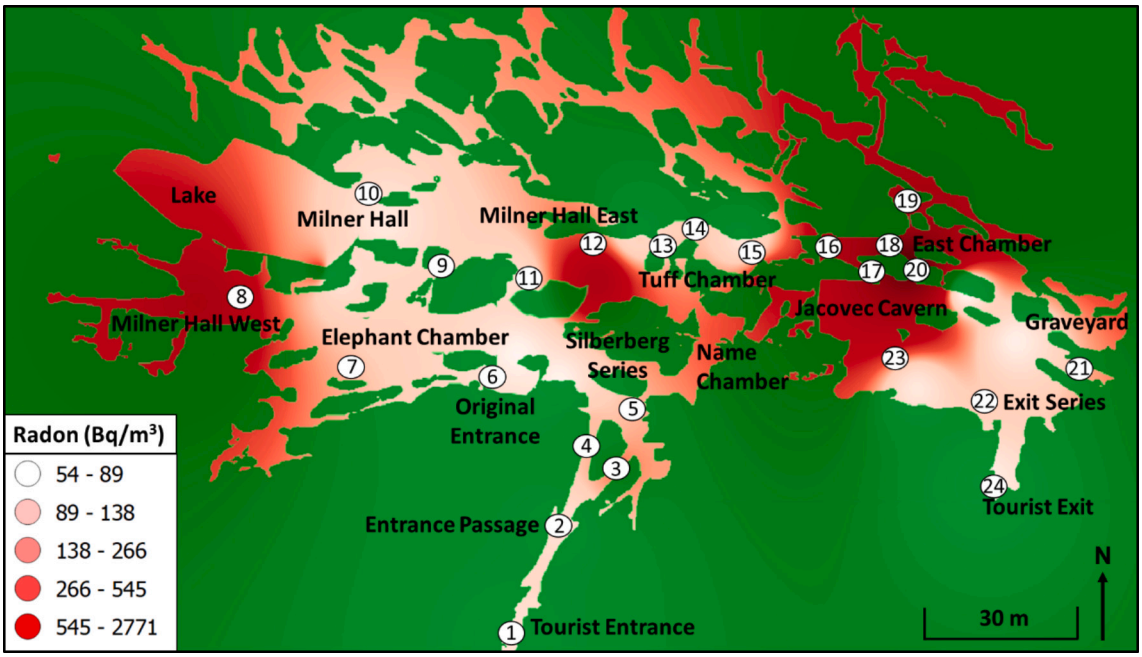

Fig. 2. A radon map of the Sterkfontein Cave with a graduated radon concentration overlay and the locations of the measurements indicated with numbers.

at least one meter away from the cave walls where possible, and on top of the geological formations.

Measurements were done at the start of February during the warmer summer months of the southern hemisphere. The EICs were left for 24 h, where after their final potentials were measured. The selection of this short timeframe stems from high radon levels typically found in caves, which could deplete the electric charge of the EICs. The measured potential difference was then used to calculate the airborne radon concentration using the expression

$$RnC = \frac{(V_i - V_f)}{(T)(CF)} - BG \quad (1)$$

where RnC represents the indoor radon concentration, V_i and V_f the initial and final electret potentials respectively, T the deployment time in days, CF a linearization coefficient (Kotrappa et al., 1990), and BG the radon concentration equivalent of natural gamma (γ) radiation background. A background radiation correction was made by assuming a typical gamma radiation of 32 Bq/m^3 (Shahbazi-Gahrouei et al., 2013). This value also correlates to a prediction by Bezuidenhout (2023) who used the geology of the area to predict a dose rate of between 50 and 100 nGy/h. Assuming a worst case of 100 nGy/h, this translates to a radon equivalent of 32 Bq/m^3 (Kotrappa et al., 1990).

2.2. Radon map

The mapping, plotting, and analysis of the data were conducted in QGIS. The measured radon values were interpolated using the Inverse Distance Weighting (IDW) interpolation method, which is available in the Processing Toolbox of QGIS. All the layers were generated as graduated red colour ramps that were divided into quartile intervals. Subsequently, the interpolated layers representing radon concentrations were superimposed onto geographic images of the Sterkfontein Cave and a lateral depiction of the Milner Hall, shown in Fig. 2 and Fig. 4.

3. Results and discussion

Fig. 2 shows the interpolated radon concentration overlay superimposed on a map of the Sterkfontein Cave. The 24 measurement locations are also indicated, with the measured radon concentration at each location listed in Table 1. The average radon concentration of 427 Bq/m^3 is also listed in the table.

As can be seen in Fig. 2, three main areas with elevated radon concentrations were identified. The first is the lowest-lying area of the cave above the subterranean lake, mainly in the confined western sections and lower parts of the Milner Hall (measurements 8 and 10 in Table 1). An average radon concentration of 1059 Bq/m^3 was measured in the western section of the Miler Hall. Radon gas is approximately 7.5 times heavier than air (Kolarž et al., 2009), and consequently tends to accumulate in low-lying areas. It is also water-soluble (Appleton, 2012), and therefore notably elevated in subterranean waters (Dimova et al., 2013). The Lake located at the bottom of the Elephant Chamber and Milner Hall therefore contributes to the emanation of radon gas into these chambers. Due to the confined space above the subterranean lake and constricted

Table 1
A list of the measured airborne radon levels at the different cave locations.

Measurement nr.	Location	Radon Concentration (Bq/m^3)
1	Tourist Entrance	157
2	Entrance Passage	168
3	Entrance Passage (Left)	371
4	Entrance Passage (Right)	307
5	Silberberg Grotto	70
6	Original Entrance	58
7	Elephant Chamber	459
8	Milner Hall West	1059
9	Elephant Chamber link tunnel	72
10	Milner Hall	119
11	Elephant Chamber link tunnel	187
12	Milner Hall East	942
13	Tuff Chamber	136
14	Tuff Chamber passage	268
15	Jacovec access passage	265
16	Jacovec access passage	139
17	Fossil Cavern	602
18	East Chamber	675
19	East Chamber (North)	1048
20	East Chamber (South)	2771
21	Graveyard	54
22	Exit Series	94
23	Graveyard (exit)	129
24	Tourist Exit	85
	Average	427

ventilation, radon concentrations are elevated in this area of the chamber. It is also the furthest from any of the openings to the surface, which further impairs ventilation.

The second area where elevated radon concentrations were measured was in the eastern part of the tourist section, denoted East Chamber, which formed within sediment that accumulated in the cavities of the denudated dolomite of the cave. Most of these sediments were found to originate from sources outside the cave and showed limited mixing with the cave earth (Stratford et al., 2014). This sedimentary fill in the karstic cavities of the cave is illustrated in Fig. 3, with the Name Chamber denoted by A. The lithology in this part of the cave is consequently different from its general karst character, due to the composition of the fill sediment. The rock in this part includes deposits of breccia with a phosphatic character (Hakl et al., 1997). Phosphatic deposits are generally accompanied by high concentrations of uranium, and its daughter nuclides, such as radon (Menzel, 1968). Elevated radon concentrations are therefore expected in this part of the cave. The diffusion and transport rate of radon in clastic sedimentary rocks like breccia is high which will also enhance radon emissions.

The eastern section of the Milner Hall (demarcated as number 12 in Fig. 2), down into the Name Chamber also demonstrated elevated radon concentrations. As can be seen in Fig. 3, this part of the cave, denoted by B, is relatively confined. Stratford et al. (Stratford et al., 2014) also found sediment flowing into this area from the Name Chamber and Silberberg Series. This section therefore contains similar fill deposits, contributing to elevated radon concentrations that are further exacerbated by poor ventilation. Consequently, as illustrated in Fig. 4, similar radon concentrations were measured in the upper and lower sections of Milner Hall.

Surficial palaeokarst deposits are also abundant above the eastern section of the cave system (indicated by the bold black line in Fig. 1), which also contained the repository where the *Australopithecus* fossils were found (Tobias, 2000). The majority of these early hominin specimens originated from subterranean deposits that built up in deep dolomitic caves, connected to the surface through avens (Moggi-Cecchi et al., 2007). The accumulation of hominin assemblages was likely influenced by factors such as large carnivores, natural traps, and slope wash (Brain, 1981). Once underground, the specimens became buried in talus deposits, solidifying into robust breccias cemented with calcite. This phosphatization process affects the uranium sorption of the material and has consequently been linked to high radioactivity (Farmer et al., 2008) (Długosz-Lisiecka et al., 2021). Since radon is part of the decay chain of uranium, this process also contributes to the elevated radon concentrations measured in the eastern part of the cave. The proportion of radon that is released directly from the soil is contingent upon both the depth at which it is generated and the permeability of the underlying earth (Gabrovsek, 2023).

Table 2 shows how the radon concentrations in the Sterkfontein Cave compared to measurements performed in other caves. Most notably, the radon concentrations of two other South African caves are also listed: the Sudwala and Cango caves. It is worth noting that the maximum radon concentration measured in the Sterkfontein Cave exceeds that of the Sudwala Cave by 948 Bq/m^3, despite many similarities between the two caves. Both caves are formed in dolomite lithologies and both maintain constant temperatures of around 18 °C. Dolomite lithologies typically have low uranium concentrations (GEOROC database, 2021).

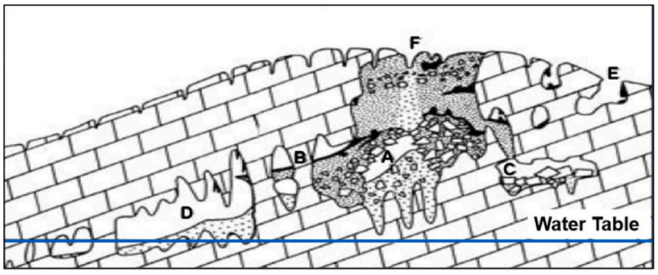

Fig. 3. A side view illustration of the Sterkfontein Cave indicating the sedimentary fill in the karstic cavities. The letters mark the fill in the Name Chamber (A), cavities between the dolomite and fill (B), Jacovec Cavern (C), Milner Hall and Elephant Chamber (D), unfilled surface cavity in the dolomite (E) and shallow hole in the decalcified breccia (F). The image was adapted from Martini et al. (Wipplinger et al., 2003).

Le Roux et al. (le Roux et al., 2023) linked the elevated radon levels in the Sudwala Cave to insufficient ventilation from its single known entrance, with cave breathing diffusing radon from deep within the cave. However, this does not apply to Sterkfontein Cave since the cave has multiple openings to the surface. Consequently, the Sterkfontein Cave is better ventilated than Sudwala. This is apparent from the low radon levels measured at both the Tourist Entrance and Exit, along with the overall low average radon concentrations. Though cave breathing is still likely to occur, the areas in the Sterkfontein Cave exhibiting increased radon concentrations result from the presence of phosphatic deposits. Though these primarily originated from the surrounding environment, the biogenic activity in the cave can also contribute to these deposits. Considering the number of openings to the surface, many cave-dwelling organisms, such as porcupines, insects, and small bat colonies, inhabit the cave. As they migrate through the cave and use different entrances for access, these organisms add to the phosphatic build-up through their diet which over time contributes to the accumulation of guano and other organic materials. The mineralization of these materials over time can also increase the phosphatic deposits found in certain cave cavities. Additionally, the subterranean lake also concentrates the radon gas in the low-lying sections of the cave.

4. Conclusions

Radon concentrations in the tourist section of the Sterkfontein cave were measured using 24 electrets ion chambers. Notwithstanding the cave's comparatively favourable ventilation conditions, elevated radon concentrations ranging from 942 Bq/m^3 to 2771 Bq/m^3 were identified in three general areas along the tourist route. Even though this was comparable to previous summer measurements in a similar South African cave, the average radon concentration was found to be 3 times less at 427 Bq/m^3. The lowest radon concentration measured in the Sterkfontein cave was also lower, a phenomenon attributed to the effective ventilation at the Tourist Entrance and Exit. The restricted ventilation in the deeper cave sections allows for the accumulation of radon gas.

Despite dolomite inherently having low uranium concentrations, elevated radon concentrations were found in the low-lying areas of the cave's tourist section. Many of these areas are characterized by phosphatic fill deposits, which are typically associated with increased radon levels. Owing to its density, radon gas also naturally tends to accumulate in low-lying areas, further exacerbating the concentrations found these areas.

Radon gas is also water soluble, leading to its dissolution in the cave's groundwater. This groundwater accumulates in a subterranean lake in the western part of the tourist section. Its low-lying location combined with radon diffusion into the confined space above the lake resulted in elevated radon concentrations being measured in this area.

The WHO stipulates 300 Bq/m^3 as a hazardous level for indoor radon, based on the occupational exposure of the inhabitant. Even though certain sections of the Sterkfontein cave exceed this level by up to 9 times, the general occupancy of the cave by tourists is quite low. Consequently, there is no discernible risk due to the limited time spent in the confined cave sections with elevated radon concentrations.

CRediT authorship contribution statement

Jacques Bezuidenhout: Writing – review & editing, Writing – original draft, Visualization, Software, Project administration,

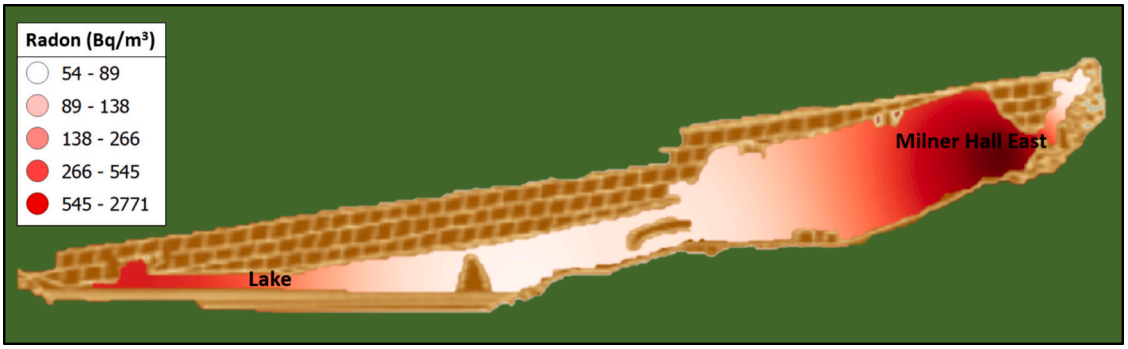

Fig. 4. A side view of the Milner Hall overlaid with a graduated interpolation of the radon concentrations. The image was added from Martini et al. (Wipplinger et al., 2003).

Table 2
A list of published radon concentrations (Bq/m^3) in various caves.

Country	Number-type of caves	Rn concentration (Bq/m^3)			References
		Min	Max	Mean	
Australia	57-show caves			6330 (annual); 500 (winter); 795 (spring)	(Solomon et al., 1996)
Greece	Perama cave			1311 (winter); 925 (summer)	(Papachristodoulou et al., 2004)
Ireland	3-show caves	488	11,285	2040; 5590; 7400	(Duffy et al., 1996)
Poland	2-caves	100	3600		(Przylibski, 1999)
Slovenia	10-caves			2350 (summer) to 27,000 (winter)	(Jovanovic, 1996)
UK	3-recreational caves	32	12,552		(Sperrin et al., 2000)
UK	Limestone	27	7800		(Gillmore et al., 1999)
North-Spain	Ultamira cave	186	7120	5562 (summer)	(Lario et al., 2005)
Venezuela	Show caves	100	80,000		(Sajohus et al., 1997)
South Africa	3-tourist and adventure	255	1822	750 (winter)	(le Roux et al., 2023)
South Africa	Limestone	800	2600	1350 (summer)	(Nemangwele, 2005)
South Africa	3-tourist and adventure	53	2770	427 (summer)	This study

Methodology, Investigation, Formal analysis, Data curation, Conceptualization. **Rikus le Roux:** Writing – review & editing, Writing – original draft, Validation, Project administration, Methodology, Investigation, Formal analysis, Data curation.

Declaration of competing interest

The authors declare no conflict of interest. This research was funded by the Centre for Nuclear Safety and Security (South Africa), project no. CNSS0117-D2-SUN.

Data availability

Data will be made available on request.

References

Appleton, J., 2012, November. Radon in air and water. In: InEssentials of Medical Geology, pp. 239–277.
Bezuidenhout, J., 2023. Estimating geothermal and background radiation hotspots from primordial radionuclide concentrations in geology of South Africa. J. Environ. Radioact. 259 (260), 107118.
Brain, C., 1981. The Hunters of the Hunted? An introduction to African Cave Taphonomy. University of Chicago Press, Chicago.
Cigno, A., 2005. Radon in Caves. Int. J. Speleol. 34 (1–2), 1–18.
Dimova, N., Burnett, W., Chanton, J., Corbett, J., 2013. Application of radon-222 to investigate groundwater discharge into small shallow lakes. J. Hydrol. 112–122.
Długosz-Lisiecka, M., Tyborowski, D., Krystek, M., 2021. Radioactive fossils: the uranium anomaly and its paleobiological implications. Chemosphere 131444 (285), 1–7.
Duffy, J., Madden, J., Mackin, G., McGarry, A., 1996. A reconnaissance survey of radon in show Cave in Ireland. J. Environ. Radioact. 49, 235–240.
Eriksson, P., Reczko, B., 1995. The sedimentary and tectonic setting of the Transvaal Supergroup floor rocks to the Bushveld complex. J. Afr. Earth Sci. 21 (4), 487–504. https://doi.org/10.1016/0899-5362(95)00111-5.
Farmer, C., Kathren, R., Christensen, C., 2008, August. Radioactivity in fossils at the Hagerman Fossil Beds National Monument. J. Environ. Radioact. 99 (8), 1355–1359.
Gabrovsek, F., 2023. How do caves breathe: the airflow patterns in karst underground. PLoS One 1–22.
GEOROC database, 2021. Geochemistry of Rocks of the Oceans and Continents. Max Planck Institute for Chemistry, Mainz, Germany. Retrieved from http://georoc.mpch-mainz.gwdg.de/georoc/ Updated.
Gillmore, G., Sperrin, M., Philips, P., Denman, A., 1999. Radon hazard, geology and exposure of cave users: a case study and some theoretical perspectives. Environ. Int. 22, S409–S413.
Hakl, J., Hunyadi, I., Varhegyi, A., 1997. Radon monitoring in caves. In: Radon Measurements by Etched Track Detectors. World Scientific, pp. 261–283.
Jovanovic, P., 1996. Radon measurement in karst Caves in Slovenia. Environ. Int. 22, 429–432.
Kolarž, P., Filipović, D., Marinković, B., 2009, November. Daily variations of indoor air-ion and radon concentrations. Appl. Radiat. Isot. 1-6.
Kotrappa, P., Dempsey, J., Ramsey, R., Stieff, L., 1990. A practical E-PERM (electret passive environmental radon monitor) system for indoor 222Rn measurement. Vol. 58(4). Health Phys. *58* (4).
Kuman, K., 1994. The archaeology of Sterkfontein - past and present. J. Hum. Evol. 471–495.
Lario, J., Sanchez, M., Canaveras, J., Cuezva, S., Soler, V., 2005. Radon continuous monitoring in Altamira Cave (North Spain) to assess user's annual effective dose. J. Environ. Radioact. 80, 161–174.
le Roux, R., Bezuidenhout, J., Nemangwele, F., 2023. Radon concentrations in the Sudwala cave. Arab. J. Geosci. 16 (4), 1–9.
Menzel, R.G., 1968. Uranium, radium, and thorium content in phosphate rocks and their possible radiation hazard. J. Agric. Food Chem. 16 (2), 231–234. Retrieved 8 23, 2023, from https://pubs.acs.org/doi/abs/10.1021/jf60156a002.
Moggi-Cecchi, J., Grine, F., Tobias, P., 2007. Early hominid dental remains from members 4 and 5 of the Sterkfontein Formation (1966-1996 excavations): catalogue, individual associations, morphological descriptions and initial metrical analysis. J. Hum. Evol. 50 (3), 239–328.
NCRP, 1988. Evaluation of Occupational and Environmental Exposures to Radon and Radon Daughters in the United States. NCRP Report N° 78.
Nemangwele, F., 2005. Radon in the Cango Caves.
Papachristodoulou, C., Ionknides, K., Stamoulis, K., Patiris, D., Pavcides, S., 2004. Radon activity levels and effective doses in the Perama cave, Greece. Health Phys. 86 (6), 619–624.

Przylibski, T., 1999. Radon concentration changes in the air of two caves in Poland. J. Environ. Radioact. 45, 81–94.
Sajohus, L., Greaves, E., Palfalvi, J., Urban, F., Merlo, G., 1997. Radon concentration measurements in Venezuelan Caves using SSNTDS. Radiat. Meas. 28 (1–6), 725–728.
Shahbazi-Gahrouei, D., Setayandeh, S., Gholami, M., 2013. A review on natural background radiation. Adv. Biomed. Res. 2 (65) https://doi.org/10.4103/2277-9175.115821.
Solomon, S., Langroo, R., Lyons, R., James, J., 1996. Radon exposure to tour guides in Australian show caves. Environ. Int. 22, 409–413.
Sperrin, M., Denman, T., Phillips, P., 2000. Stimating the dose from radon to recreational cave users in the Mendips, UK. J. Environ. Radioact. 49 (2), 235–240.
Stratford, D., 2015. In: Grab, S., Knight, J., Grab, S., Knight, J. (Eds.), Landscapes and Landforms of South Africa, 17. World Geomorphological Landscapes, Cham, Switzerland, pp. 147–153.
Stratford, D., 2017. A review of the geomorphological context and stratigraphy of the Sterkfontein Caves, South Africa. Hypogene Karst Regions and Caves of the World 879-891. https://doi.org/10.1007/978-3-319-53348-3_60.
Stratford, D., Grab, S., Pickering, T.R., 2014, August. The stratigraphy and formation history of fossil- and artefact-bearing sediments in the Milner Hall, Sterkfontein Cave, South Africa: New interpretations and implications for palaeoanthropology and archaeology. J. Afr. Earth Sci. 96, 155–167.
Tanner, A.B., 1978. Radon migration in the ground: a supplementary review. In: Natural Radiation Environment III, pp. 5–56. CONF-780422.
Thackeray, J., 2020. A summary of the history of exploration at the Sterkfontein Caves in the Cradle of Humankind World Heritage Site. In: Zipfel, B., Richmond, B.G., Ward, C.V. (Eds.), Hominin Postcranial Remains from Sterkfontein, South Africa. Oxford University Press, Oxford, pp. 1936–1995.
Tobias, P., 2000. The fossil hominids. Oxf. Monogr. Geol. Geophys. 40, 252–276.
Wilkinson, J.M., 1983. Geomorphic Perspectives on the Sterkfontein Australopithecine Breccias. J. Archaeol. Sci. 515–529.
Wipplinger, P.E., Moen, H.F., Keyser, A., Martini, J.E., 2003. Contribution to the Speleology of Sterkfontein Cave, Gauteng Province, South Africa. Int. J. Speleol. 43–69.